# Interaction of a Synthetic Amphiphilic Polypeptide and Lipids in a Bilayer Structure†

James H. Davis,* Donna M. Clare, Robert S. Hodges, and Myer Bloom

ABSTRACT: A unique model-membrane system composed of synthetic amphiphilic peptides, as models of membrane proteins, and lipid molecules in lamellar dispersions has been studied by circular dichroism, differential scanning calorimetry, low-angle X-ray diffraction, and $^1H$ and $^2H$ nuclear magnetic resonance. The results indicate that the interactions among all the different components of the system, lipid/peptide/counterion/water, must be considered in order to understand the phase behavior. Incorporation of the peptides into the lipid bilayer transforms the three-phase line, or phase transition, of 1,2-dipalmitoyl-*sn*-glycero-3-phosphocholine (DPPC) into a broad two-phase region. In the case of potassium palmitate/peptide multilamellar dispersions at a molar ratio of 100:1, this is accompanied by an approximately 30% increase in average hydrocarbon chain order whereas this increase is only approximately 5% for DPPC/peptide bilayers at a 43:1 molar ratio. The systematic modification of the structure and composition of these systems and detailed analysis of the effects observed are expected to lead to a model for lipid–protein interactions in biological membranes.

Numerous nuclear magnetic resonance (NMR)[1] spectroscopic studies have examined the perturbation of lipid orientational order due to the interaction with protein in reconstituted and natural membranes (Davis, 1983; Devaux, 1983; Jacobs & Oldfield, 1981; Seelig & Seelig, 1980). This approach to the question of the protein–lipid interaction has been popular because NMR already provided an accurate and detailed description of phospholipid orientational order in pure lipid/water systems. NMR spectra are sensitive to the orientationally averaged order at the nuclear position, and any perturbation to the degree of orientational averaging occurring over the spectroscopic time scale will be reflected in the spectrum.

In order to carry out a systematic investigation of protein–lipid interactions by NMR, it is necessary to prepare large quantities of membrane protein. Even then, the NMR experiments, which may include relaxation measurements as a function of protein concentration and sample temperature, may require extensive signal averaging. Finally, the interpretation of the experimental results is limited by our incomplete knowledge of membrane-protein structure and by our inability to systematically modify that structure. [See, e.g., Henderson (1981) and McLachlan & Henderson (1980) for a discussion of intrinsic membrane-protein structure.]

As a first step toward the solution of this problem, we are attempting to simplify the system by constructing model membranes from synthetic amphiphilic peptides and synthetic lipids. The polypeptide is constructed with hydrophilic amino acid residues at each end and a central core of hydrophobic amino acids whose linear dimension, assuming an $\alpha$-helical structure, is designed to span the lipid bilayer.

Studies in synthetic water-soluble random copolymers containing L-leucine show that leucine is a strong $\alpha$-helix former, this tendency being attributed to hydrophobic interactions (Alter et al., 1972). Similarly, the predictive method of Chou & Fasman (1977) rates both alanine and leucine as strong $\alpha$-helix formers. Thus, poly(L-leucine) seemed to be the ideal choice for incorporation into lipid bilayers, the greater hydrophobic interaction of leucine with the bilayer interior providing greater $\alpha$-helix stability than that obtainable with alanine.

For 1,2-dipalmitoyl-*sn*-glycero-3-phosphocholine (DPPC) in excess water, the width of the hydrophobic region of the bilayer has been reported to be approximately 33 Å in the liquid-crystalline ($L_\alpha$) phase and about 47 Å in the gel ($L_\beta$) phase [see p 38 in Seelig & Seelig (1980)]. There is some uncertainty in defining the boundary between the hydrophobic and polar parts of the bilayer. Lewis & Engelman (1983) have interpreted their X-ray diffraction results to yield a width of about 26 Å for the hydrophobic region of DPPC in the $L_\alpha$ phase. We believe that this difference in widths is not due to a disagreement between X-ray and neutron-diffraction experiments but represents a different choice of the polar–hydrophobic boundary. A peptide segment consisting of 24 leucine residues in an $\alpha$-helical conformation (with a residue translation of 1.5 Å per residue) would span the liquid-crystalline phase bilayer. To maintain the transbilayer orientation, charged amino acid residues (lysine) were attached to each end of the peptide. In the first batch of peptide synthesized (peptide 1), an alanine residue was placed at one end while in the second batch (peptide 2), in addition to this alanine residue, a glycine residue was added at the other end to aid in the quantitative analysis of the purity of the final product.

The synthesis was carried outby the solid-phase stepwise procedure with poly(styrene-*co*-1% divinylbenzene)-benzhydrylamine hydrochloride resin. This support was chosen because of the high stability of the C-terminal attachment to the support during acid cleavage with 50% trifluoroacetic acid

† From the Biophysics Interdepartmental Group and the Guelph-Waterloo Program for Graduate Work in Physics, Guelph Campus, University of Guelph, Guelph, Ontario N1G 2W1, Canada (J.H.D.), the Department of Biochemistry and the Medical Research Council Group in Protein Structure and Function, University of Alberta, Edmonton, Alberta T6G 2H7, Canada (D.M.C. and R.S.H.), and the Department of Physics, University of British Columbia, Vancouver, British Columbia V6T 1W5, Canada (M.B.). *Received March 10, 1983.* This research was supported by the Natural Sciences and Engineering Research Council of Canada (J.H.D. and M.B.) and by the Medical Research Council of Canada (R.S.H.).

[1] Abbreviations: NMR, nuclear magnetic resonance; DPPC, 1,2-dipalmitoyl-*sn*-glycero-3-phosphocholine; $L_\alpha$, lamellar liquid-crystalline phase; $L_\beta$, lamellar gel phase with long molecular axis parallel to bilayer normal; Boc, *tert*-butyloxycarbonyl; DCC, dicyclohexylcarbodiimide; TFA, trifluoroacetic acid; DEA, diisopropylethylamine; DSC, differential scanning calorimetry; CD, circular dichroism; DPPC-$d_{62}$, 1,2-bis(perdeuteriopalmitoyl)-*sn*-glycero-3-phosphocholine; K-palmitate-$d_{31}$, potassium perdeuteriopalmitate; PC, *sn*-glycero-3-phosphocholine.

0006-2960/83/0422-5298$01.50/0 © 1983 American Chemical Society

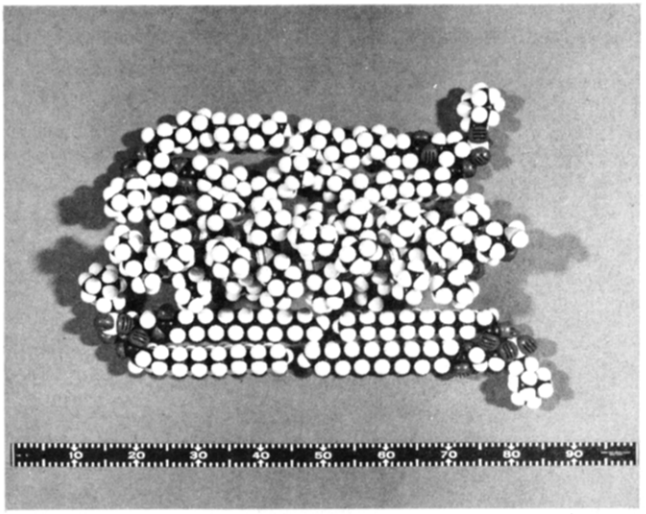

FIGURE 1: Comparison of dimensions of peptide 1 ($K_2L_{24}K_2A$-amide) and DPPC in conformations characteristic of $L_\alpha$ or liquid-crystalline phase (top) and $L_\beta$ phase (bottom). The scale factor for the molecular models is 1.25 cm/Å.

of the $N^\alpha$ protecting group (Boc), thus preventing chain loss during synthesis. On HF cleavage of the peptide from the support, the C-terminal amide is obtained directly. The amide blocks the $\alpha$-carboxyl group of the peptide, leaving only positive charges at each end of the molecule, with acetate counterions. The final product obtained was $Lys_2$-$Leu_{24}$-$Lys_2$-Ala-amide ($K_2L_{24}K_2A$-amide) for peptide 1 and $Lys_2$-Gly-$Leu_{24}$-$Lys_2$-Ala-amide ($K_2GL_{24}K_2A$-amide) for peptide 2.

We have begun our systematic investigation of this system with $^2H$ NMR measurements of 1,2-bis(perdeuteriopalmitoyl)-*sn*-glycero-3-phosphocholine/peptide at a weight ratio of 10:1 dispersed in an equal weight of water. This corresponds to a lipid to peptide molar ratio of 43:1. X-ray diffraction and differential scanning calorimetry (DSC) have been used in conjunction with NMR to provide a quantitative description of the phase behavior of the samples. Figure 1 illustrates the relative dimensions of peptide 1 and the DPPC bilayer in the $L_\alpha$ (top) and $L_\beta$ (bottom) phases. The scale is in centimeters and the conversion factor for the molecular models is 1.25 cm/Å.

We have also examined mixtures of potassium palmitate/peptide at molar ratios of 100:1 and 200:1 dispersed in $^2H_2O$ at a soap/peptide to water weight ratio of 70:30, corresponding to the degree of hydration giving a lamellar phase in the pure soap/water systems. The $^2H$ NMR spectra of the perdeuterated soap have been studied as a function of temperature, encompassing the $L_\alpha$ to $L_\beta$ phase transition.

Both of these studies indicate a strong sensitivity of the lipid phase behavior to the presence of the peptide. Analysis of the two-phase regions that occur can provide quantitative information on the peptide–lipid interaction.

## Experimental Procedures

*Materials.* All chemicals and solvents used in the peptide synthesis were reagent grade. Picric acid, from Matheson Coleman and Bell, NJ, was dissolved in dichloromethane and dried over $MgSO_4$ before use (Hodges & Merrifield, 1975a). Dichloromethane was distilled over $CaCO_3$; diisopropylethylamine (DEA) was distilled first over NaH and then over ninhydrin prior to use. Poly(styrene-*co*-1% divinylbenzene)-benzhydrylamine hydrochloride resin (0.51 mmol of $NH_2$/g of resin) was purchased from Beckman Instruments, Palo Alto, CA. Boc-amino acids purchased from Protein Research Foundation, Japan, and Bachem Fine Chemicals, Torrance, CA, were used without further purification. Dicyclohexylcarbodiimide (DCC) was obtained from Pierce, Rockford, IL.

*Peptide Synthesis.* The 30-residue peptide was synthesized by using the general procedures for solid-phase peptide synthesis on a Beckman peptide synthesizer Model 990. The COOH-terminal amino acid, Boc-Ala (0.5 mmol in 10 mL of $CH_2Cl_2$), was coupled to benzhydrylamine resin (2 g; 0.51 mmol of $NH_2$/g of resin) with one dicyclohexylcarbodiimide-mediated coupling (0.5 mmol of DCC in 5 mL of $CH_2Cl_2$). The Boc-Ala resin was acetylated by a 60-min treatment with pyridine/acetic anhydride/benzene (3:1:3 v/v, 25 mL/g of amino acid resin) after being prewashed for 5 min with the same mixture. This treatment terminated the free amino groups on the benzhydrylamine resin that did not couple Boc-Ala. The substitution of alanine on the resin was determined to be 0.20 mmol/g of resin by picrate monitoring (Hodges & Merrifield, 1975a) before and after coupling, after acetylation and deprotection of the Boc group. All amino groups were protected at the $\alpha$-amino position with the Boc group, and the following side-chain blocking group was used for lysine: [(2-chlorobenzyl)oxy]carbonyl. Boc-amino acids (1.2 mmol, 3 equiv) in 10 mL of $CH_2Cl_2$ were added to the peptide resin followed by 5 mL of DCC in $CH_2Cl_2$ (1.2 mmol). Double couplings of 60 min each were performed at each step of the synthesis. The Boc group was removed at each cycle of the synthesis by treatment with 40 mL of 50% trifluoroacetic acid (TFA)/$CH_2Cl_2$ (v/v) with a double-deprotection program of 30 min each. Following the double-deprotection, neutralization was carried out with 40 mL of 5% diisopropylethylamine/$CH_2Cl_2$ (v/v) prior to coupling.

The program used for the attachment of each amino acid consisted of two cycles. Deprotection cycle: 50% TFA/$CH_2Cl_2$, 1 min; 50% TFA/$CH_2Cl_2$, 30 min; $CH_2Cl_2$, 4 times, 1 min; 80% 2-propanol/$CH_2Cl_2$, 2 times, 1 min; $CH_2Cl_2$, 8 times, 1 min; repeat of the deprotection cycle. Coupling cycle: 5% DEA/$CH_2Cl_2$, 3 times, 2 min; $CH_2Cl_2$, 7 times, 1 min; Boc-amino acid, 5 min; DCC, 60 min; $CH_2Cl_2$, 3 times, 1 min; 80% 2-propanol/$CH_2Cl_2$, 2 times, 1 min; $CH_2Cl_2$, 2 times, 1 min; 80% 2-propanol/$CH_2Cl_2$, 2 times, 1 min; $CH_2Cl_2$, 8 times, 1 min; repeat of the coupling cycle. The $CH_2Cl_2$ and 2-propanol washes were 75 and 40 mL, respectively. The picrate-monitoring program was used only to determine the substitution level of Boc-Ala and has been previously described (Hodges & Merrifield, 1975a).

Amino acid analyses on the acid hydrolysates of the peptide–resin were performed at various stages in the synthesis on a Durrum D-500 amino acid analyzer. The peptide–resin was hydrolyzed in a mixture of methanesulfonic acid/propionic acid/water (0.5 mL:1.2 mL:0.3 mL) for 72 h at 110 °C as previously described (Hodges & Merrifield, 1975b).

*Cleavage of Peptide from Resin.* The cleavage of the peptide from the resin support and removal of blocking groups were carried out in hydrofluoric acid at 0 °C for 45 min in a type 1 hydrofluoric acid apparatus from Protein Research Foundation with 10% anisole (v/v) as a scavenger for cations.

The HF and the bulk of the anisole were then removed under vacuum below 0 °C, and the residual anisole and byproducts were extracted with ether. The cleaved peptide was extracted from the resin with 25% trifluoroacetic acid/$CH_2Cl_2$ and removed from the resin by filtration. The trifluoroacetic/$CH_2Cl_2$ solution was evaporated to dryness and the peptide dissolved in a minimal volume of 50% acetic acid. This solution was diluted with water to 5% acetic acid and lyophilized. Acid hydrolysis was performed on the peptide, with the procedure described above for resin hydrolysis, or in 6 N

HCl. However, it was subsequently found that longer periods (5 days) of hydrolysis improved the reproducibility of the amino acid analysis. Due to the high levels of leucine in the peptide, diluted and concentrated aliquots of the hydrolysates were taken for amino acid analysis. The following results were obtained for peptide 2 ($K_2GL_{24}K_2A$-amide): concentrated sample, Gly (0.98), Ala (1.07), Lys (3.97), Leu (off scale); dilute sample, Gly (1.02), Ala (1.07), Lys (4.28), Leu (23.64). The formula weights of the two peptides with acetate counterions are as follows: peptide 1, 3612; peptide 2, 3669.

*Sample Preparation.* Potassium palmitate was prepared from palmitic acid (Calbiochem, La Jolla, CA) that has been perdeuterated following the procedure of Hsiao et al. (1974). 1,2-Bis(perdeuteriopalmitoyl)-*sn*-glycero-3-phosphocholine was from the same batch used by Davis (1979) obtained from Lipid Specialties, Boston, MA, or was synthesized in our laboratory according to the method of Gupta et al. (1977).

Peptide 1, as prepared above, exhibited limited solubility in methanol. To increase its solubility, a drop of TFA was added to the peptide/methanol suspension after which the mixture immediately became transparent. The methanol/peptide solution was evaporated to dryness and pumped at room temperature for at least 8 h to remove all traces of methanol and any excess TFA or acetic acid. The peptide and lipid were mixed in the appropriate ratio in methanol, which was then removed by evaporation. The lipid/peptide mixture was then pumped dry for at least 8 h. The NMR, DSC, and X-ray diffraction samples were prepared by adding either $^1H_2O$, $^2H_2O$, or 50 mM potassium phosphate buffer at pH 7.0 at appropriate concentrations and mixing either by hand with a glass stirring rod (DSC and X-ray) or by centrifugation back and forth in sealed ampules (NMR samples). Thin-layer chromatography indicated that the DPPC/peptide samples were free of lyso-PC before the experiments and that there had been little or no degradation of the sample during the course of the experiments. To investigate the cause of the observed phase behavior, samples of peptide 2 used for DSC were prepared with and without the TFA treatment described above.

*Circular Dichroism (CD).* CD measurements were made on a Cary 60 spectropolarimeter with a 6001 CD attachment and water-cooled lamp housing. The percentage $\alpha$-helix can be calculated on the basis of the theoretical value, as described by Chen et al. (1974), for $[\theta]_{220}$ of $-33\,154$ deg·cm$^2$·dmol$^{-1}$ for a 100% $\alpha$-helical peptide of 30 residues. The CD spectrum was obtained for the peptide in methanol at a concentration of 0.621 mg/mL (as determined by amino acid analysis).

*Differential Scanning Calorimetry (DSC).* Calorimetry was performed on typically a few milligrams of lipid/peptide mixture in water or buffer in a Microcal MC-2 high-sensitivity differential scanning calorimeter (Microcal, Inc., Amherst, MA). Scan rates were slower than 45 °C/h.

*X-ray Diffraction.* Low-angle X-ray diffraction measurements were performed on a linear position sensitive detector. The samples were in 1 mm diameter quartz capillary tubes inserted into a variable-temperature chamber whose temperature could be set and controlled to better than ±0.5 °C. Typical exposure times were 30 min.

*Nuclear Magnetic Resonance.* High-resolution proton ($^1H$) NMR measurements were obtained, with Fourier transform techniques on the Bruker WH-400 NMR spectrometer operating at 400.0 MHz for protons in the Department of Chemistry at the University of British Columbia. All experiments were performed with spinning sample tubes at the ambient temperature of the probe.

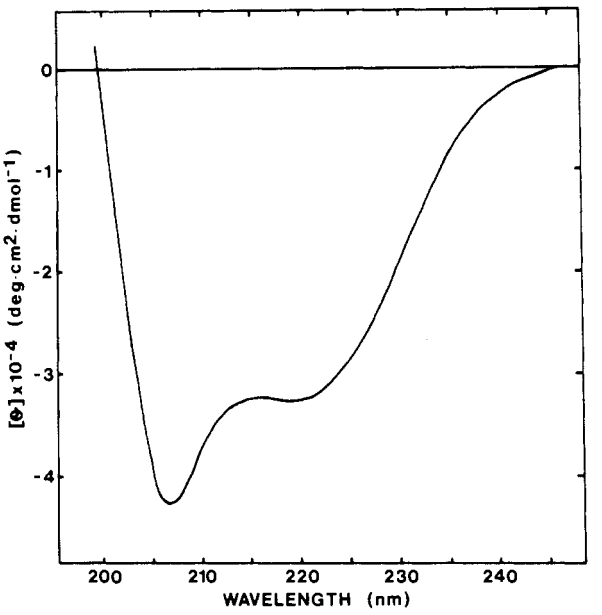


FIGURE 2: Circular dichroism spectrum of synthetic peptide 1 ($K_2L_{24}K_2A$-amide) in methanol at 27 °C. The peptide concentration was 0.618 mg/mL. A similar spectrum was obtained for peptide 2 ($K_2GL_{24}K_2A$-amide).

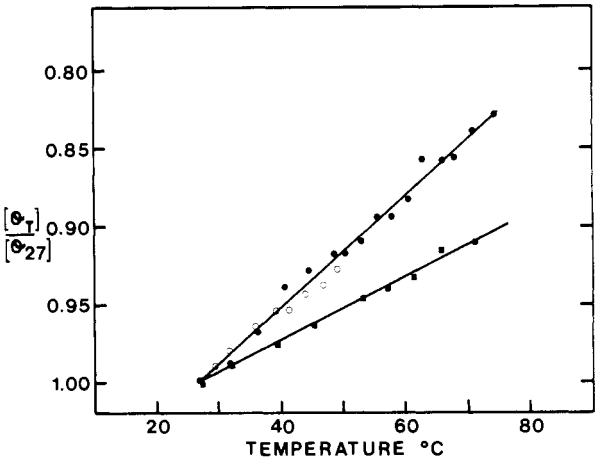


FIGURE 3: Temperature dependence of ratio of mean residue ellipticity at 222 nm to that at 27 °C, denoted by $[\theta_T]/[\theta_{27}]$, for peptide 2 ($K_2GL_{24}K_2A$-amide) in methanol (○), 1-propanol (●), and 1% Ammonyx LO (a nondenaturing detergent) (■).

The $^2H$ NMR spectra were obtained at 37.2 MHz on a Bruker SXP 100 spectrometer. The quadrupolar echo (Davis et al., 1976) was formed by using two 90° pulses of 5.0-$\mu$s length separated by a time delay of 60 $\mu$s at a repetition rate of 2 s$^{-1}$.

## Results

*Circular Dichroism.* The CD spectrum of a dilute solution of $K_2L_{24}K_2A$-amide (peptide 1) in methanol is shown in Figure 2. Similar spectra were obtained for $K_2GL_{24}K_2A$-amide in methanol and for both peptides in solutions of 1-propanol and the nondenaturing detergent Ammonyx LO. The characteristics of the spectra between about 200 and 240 nm are typical of those obtained for the $\alpha$-helical conformation of polypeptides (Chen et al., 1974), and the value of $[\theta]$ at 222 nm corresponds to the 29-residue peptide being about 90% helical at 27 °C. As may be seen from Figure 3, the fractional helicity decreases linearly with temperature between 27 and 75 °C, changing by about 17% for methanol and 1-propanol solutions and 10% for the 1% Ammonyx LO solution.

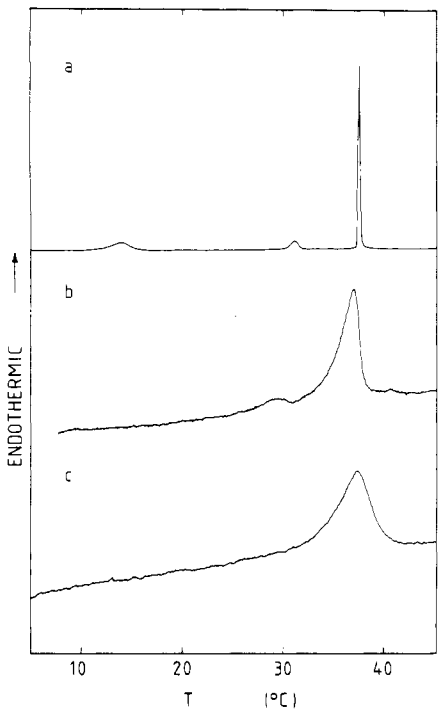


FIGURE 4: Differential scanning calorimetry plots for increasing temperature. Scan rate for (a) was 7 °C/h while for (b) and (c) the scan rate was less than 35 °C/h. All scans shown were for samples in excess of 50 mM potassium phosphate buffer at pH 7.0. (a) DPPC-$d_{62}$; (b) DPPC-$d_{62}$/peptide 2, 44:1 molar ratio, with acetate counterions; (c) DPPC-$d_{62}$/peptide 2, 44:1 molar ratio, but where peptide had TFA counterions.

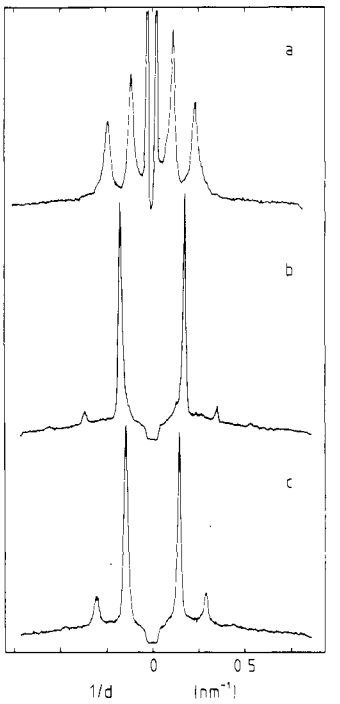


FIGURE 5: Low-angle X-ray diffraction patterns from DPPC/peptide 2 mixtures: (a) a DPPC/peptide 2 molar ratio of 44:1, at 50 °C in 50% $H_2O$, by weight; (b) a DPPC-$d_{62}$/peptide 2 50:1 molar ratio at 50 °C, in 57% (by weight) phosphate buffer, 50 mM, at pH 7.0; and (c) same sample as in (b) but at 35 °C.

*Differential Scanning Calorimetry.* Figure 4a is a DSC scan at 7 °C/h of 9 mg of pure DPPC-$d_{62}$ in excess potassium phosphate buffer, 50 mM, pH 7.0. The main-chain melting transition at 37.5 °C, the pretransition near 31 °C, and the subtransition near 14 °C (Chen et al., 1980) are all clearly evident. A DSC scan of 6.3 mg of DPPC-$d_{62}$/peptide 2 with acetate counterions in excess phosphate buffer, lipid to peptide weight ratio of 10:1 (corresponding to a molar ratio of 44:1), is shown in Figure 4b. The main-phase transition, at 37.5 °C in the pure lipid is broadened to lower temperatures, suggesting a wide two-phase coexistence region. The small broad peak near 30 °C may be the pretransition. The large asymmetric peak and the small peak at 30 °C are reproducible and independent of the amount of buffer present (from equal weights of lipid/peptide mixture and buffer to a 30-fold excess of buffer). When distilled $H_2O$ was used instead of buffer, identical results were obtained.

The bottom scan, Figure 4c, is for a sample of DPPC-$d_{62}$/peptide 2 at a lipid to peptide weight ratio of 10:1 in excess phosphate buffer, 50 mM, pH 7.0, where the peptide had been solubilized in methanol with TFA, as described earlier. In this case, the broad asymmetric peak corresponding to the main-phase transition of the lipid extends both above and below the transition temperature of the pure lipid. This behavior was also observed for samples in distilled $H_2O$ instead of phosphate buffer. These calorimetric results are in complete agreement with the X-ray diffraction and $^2H$ NMR results.

*X-ray Diffraction.* Low-angle X-ray diffraction measurements on samples of DPPC-$d_{62}$/peptide 2 (at 50:1 molar ratio) with acetate counterions in water reveal a dependence of the total bilayer repeat spacing on water concentration similar to that observed for multilayers of charged lipids (Jahnig et al., 1979). When potassium phosphate buffer is used instead of distilled water, the bilayer spacing is independent of buffer concentration at least for concentrations greater than 50% weight buffer. The X-ray diffraction patterns of Figure 5a,b illustrate this effect. In Figure 5a, the first-order peak spacing corresponds to a bilayer repeat spacing of ~84 Å at 50 °C for the sample in 50% water (by weight). The pattern in Figure 5b gives a bilayer repeat spacing of ~56 Å at 50 °C for a sample in 57% phosphate buffer (by weight).

Below 38 °C, the repeat spacing of the sample in buffer increases to ~70 Å, Figure 5c is at 35 °C, while that of the water sample decreases to approximately the same value. The diffraction patterns for pure DPPC-$d_{62}$ in water or buffer show no dependence on concentration above 50% (by weight) and agree with one another.

Low-angle diffraction patterns of K-palmitate-$d_{31}$/peptide 1 (100:1 molar ratio) in water (70:30 weight ratio) give a repeat spacing at 50 °C of 40.7 Å compared to a spacing of 38.2 Å for pure K-palmitate-$d_{31}$ in water (70:30 weight ratio) at that temperature. The positions of the second- and third-order peaks in the pattern are consistent with a lamellar structure.

*Nuclear Magnetic Resonance.* (*A*) *$^1H$ NMR of Peptide 2 in Methanol.* The high-resolution $^1H$ NMR spectrum of a 1.4 mg/mL solution of $K_2GL_{24}K_2A$-amide (peptide 2) in deuterated methanol provided a convenient check on the results of amino acid analysis. Assignments of the resonance lines were made on the basis of the paper by McDonald & Phillips (1969). All of the protons in the peptide were accounted for by these assignments except for the protons of the glycine residue. Analysis of the areas of the resolved lines of the $^1H$ NMR spectrum gave results for the ratios of the different amino acids in agreement with those obtained on an amino acid analyzer. The $^1H$ NMR method has the advantage over amino acid analysis of being nondestructive, but the accuracy of about ±15% obtained in our NMR experiments was poorer.

(*B*) *$^2H$ NMR of DPPC-$d_{62}$/Peptide 1.* $^2H$ NMR spectra of a sample of DPPC-$d_{62}$/peptide 1 (43:1 mole ratio) with TFA counterions in $H_2O$ (50% by weight) are shown in Figure

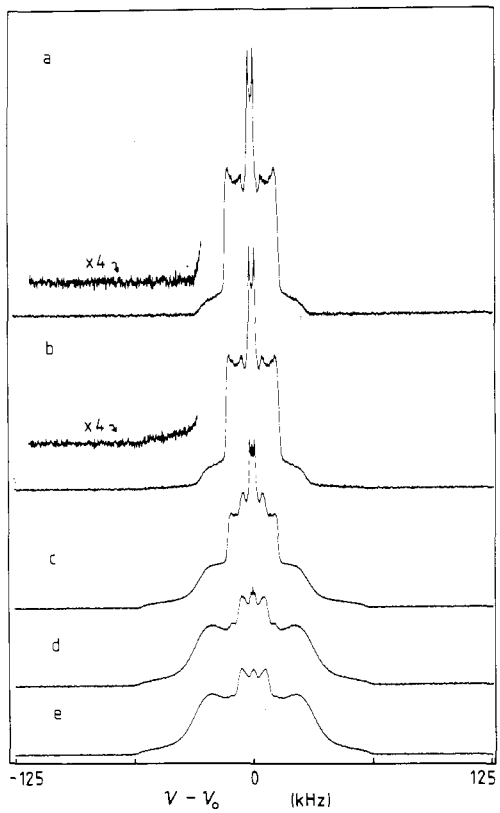


FIGURE 6: $^2H$ NMR spectra of DPPC-$d_{62}$ in DPPC-$d_{62}$/peptide 1 sample at a molar ratio of 43:1 in 50% $H_2O$, by weight. The spectra were taken at 37.2 MHz at temperatures of (a) 44, (b) 43, (c) 39, (d) 26, and (e) 20 °C. The areas of these spectra have been normalized. The out-of-phase channel, by use of quadrature detection, contains no useful information and, when the spectrometer is properly adjusted, the noise there can be replaced by zeros. On Fourier transformation, this procedure leads to perfectly symmetric spectra, as shown here.

6. At 44 °C and above the $^2H$ NMR spectra, Figure 6a, are spectra typical of a lamellar liquid-crystalline phase (Davis, 1979). If one defines the normalized spectral line shape at a temperature $T$ by $F(\omega,T)$, the $n$th moment of the spectrum, $M_n(T)$, is given by (Davis, 1979)

$$M_n(T) = \int_0^\infty \omega^n F(\omega,T)\, d\omega \qquad (1)$$

The first moment of the spectrum, $M_1$, which is proportional to the average quadrupolar splitting (Davis, 1979) at 44 °C, is $M_1 = 4.90 \times 10^4$ s$^{-1}$, compared to the value of $M_1 = 4.66 \times 10^4$ s$^{-1}$ for pure DPPC-$d_{62}$ in water (50% by weight). Just below 44 °C, the sample enters a two-phase region consisting of liquid-crystalline and gel phases, as indicated in the spectra of Figure 6b–d. These spectra are superpositions of two components, one of the form of Figure 6a, characteristic of the liquid-crystalline phase, and the other like the spectrum in Figure 6e, characteristic of the lower temperature, more-ordered gel phase.

The temperature dependence of the first moment of the spectrum is compared to that of the first moment of the spectra of pure DPPC-$d_{62}$/$H_2O$ (Davis, 1979) in Figure 7. The onset of the phase-transition region is shifted upward from 37 to 43 °C in the presence of peptide 1 with TFA counterions, in agreement with the observations made with DSC. Below 37 °C, the DPPC-$d_{62}$/peptide 1 sample still exhibits a two-component (two-phase) spectrum down to 22 °C, as may be seen from Figure 6d.

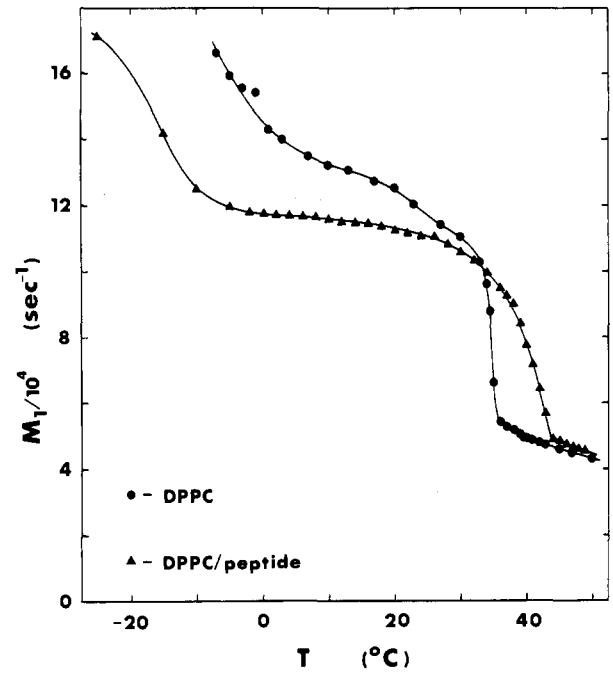


FIGURE 7: First moment, $M_1$, of $^2H$ NMR spectrum vs. temperature. The circles, for pure DPPC-$d_{62}$ in $H_2O$, are from Davis (1979), and the triangles are for DPPC-$d_{62}$/peptide 1 at a 43:1 molar ratio in 50% $H_2O$ by weight.

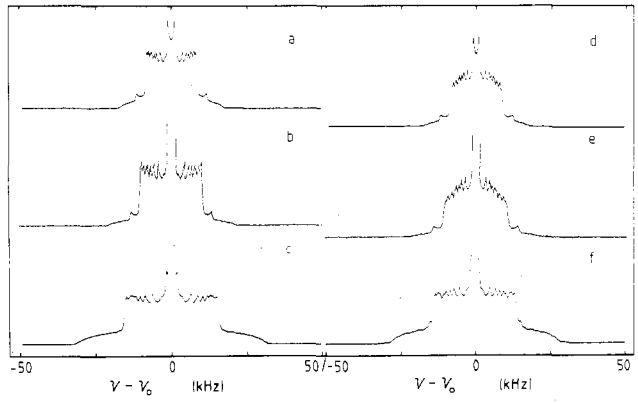


FIGURE 8: $^2H$ NMR spectra of mixtures of K-palmitate-$d_{31}$/peptide 1: (a) pure K-palmitate-$d_{31}$ at 49 °C in 30% $^1H_2O$, by weight; (b) K-palmitate-$d_{31}$/peptide 1 at a 200:1 molar ratio, at 49 °C in 30% $^2H_2O$, by weight; (c) the sample in (b) at a 100:1 molar ratio, at 49 °C in 30% $^2H_2O$, by weight; (d) the sample in (a) at 65 °C; (e) the sample in (b) at 45 °C; (f) the sample in (c) at 65 °C.

*(C) $^2H$ NMR of K-palmitate-$d_{31}$/Peptide 1.* Figure 8 shows spectra of K-palmitate-$d_{31}$ with no peptide (Figure 8a), at a mole ratio of 200:1, K-palmitate to peptide-1 (Figure 8b), and at a mole ratio of 100:1 (Figure 8c), all in 30% water, by weight (either in $^2H_2O$, Figure 8b,c, or in $^1H_2O$, Figure 8a), and at 49 °C, within the lamellar liquid-crystalline phase. The most obvious difference in these spectra is the increase in quadrupolar splitting as peptide concentration is increased. The first moment of these spectra changes from a value of $M_1 = 3.3 \times 10^4$ s$^{-1}$ for the pure K-palmitate/water sample to $M_1 = 4.0 \times 10^4$ s$^{-1}$ for the 100:1 mole ratio. Corresponding spectra for these three samples at 65 °C are shown in Figure 8d–f.

At 47 °C, the 100:1 mole ratio sample has a two-component spectrum, indicating the coexistence of gel and liquid-crystalline phases. At the 200:1 concentration, the sample does not begin its liquid-crystalline to gel transition until just below 43 °C while the pure K-palmitate-$d_{31}$ sample is in the liq-

uid-crystalline phase until the temperature is lowered to 41 °C (Davis & Jeffrey, 1977).

## Discussion

Of the various measurements reported here, only the circular dichroism is characteristic primarily of peptide conformation. The observation, Figures 2 and 3, that the peptide is predominantly $\alpha$-helical in solution is not surprising in view of the fact that poly(L-leucine) is such a strong helix former (Alter et al., 1972). It is noteworthy that the slope of the linear variation of $[\theta_T]/[\theta_{27}]$ with temperature is significantly smaller for the peptide in detergent solution than in methanol or 1-propanol. Undoubtedly, the reason for this is that the peptide is incorporated into the detergent micelles in the Ammonyx LO solution, with the hydrophobicity of the micelle interior acting to stabilize the peptide's $\alpha$-helical conformation. Preliminary CD measurements of these peptides incorporated into vesicles of both DPPC and egg yolk PC also gave spectra like that of Figure 2, characteristic of an $\alpha$-helical conformation. Furthermore, there was no measurable temperature dependence of $[\theta_T]/[\theta_{27}]$ over the same temperature range as that reported in Figure 3, even though this range encompasses the DPPC gel to liquid-crystalline phase-transition temperature. This increased stability of the peptide's helical structure indicates that the peptide is closely associated with the lipid structures. However, we have not yet established conclusively that the peptide spans the bilayer as suggested by Figure 1.

The other techniques used here are sensitive primarily to the properties of the lipids and to the thermodynamic properties of the combined lipid/peptide/counterion/water system. It is clear from our results that in order to understand the behavior of these systems, the interactions among all of these components must be considered.

The DSC results, Figure 4, show that the addition of peptide, at a molar ratio of 44 lipids per peptide, results in a broadening of the main-phase transition into a two-phase region. When the peptide is solubilized in methanol with TFA before being mixed with DPPC, the phase behavior is significantly altered. Without the TFA treatment, the entire two-phase region is below the temperature of the pure DPPC phase transition. With TFA, the two-phase region extends on both sides of the pure lipid's transition temperature. In addition, the phase behavior observed calorimetrically is independent of buffer concentration, at least above 50% buffer by weight, and is the same when distilled water is used instead of buffer. The physical origin of the different phase behavior induced by TFA is not yet understood and further investigation is under way.

The X-ray diffraction measurements we have made do not give a quantitative description of the two-phase region but do firmly establish the existence of a lamellar structure. In addition, the variation in total bilayer spacing with water concentration and the absence of any such concentration dependence when buffer is used instead of water provide strong evidence that the bilayers are charged because of the presence of the peptide. This also has implications for the phase behavior of the system since, when using water, the maximum degree of hydration is greatly increased by the presence of charge on the bilayers. In this case, it may be difficult to achieve complete and uniform hydration of the system. When buffer is used, no such problem occurs.

The $^2$H NMR results reported here, Figures 6 and 7, and some preliminary results on samples where the peptide had not been treated with TFA are in complete agreement with the DSC and X-ray diffraction measurements. In particular, the $^2$H NMR spectra of the lipid/peptide samples indicate a broad two-phase region that, in the case of TFA-treated peptide, brackets the pure lipid transition temperature. Clearly, a detailed description of the phase behavior of this system will require a more systematic study as a function of peptide concentration. However, the sensitivity of the $^2$H NMR spectrum to the phase behavior, i.e., the great difference between the spectrum of lipids in the liquid-crystalline phase and that of lipids in the gel phase, enables us to quantify the state of the system as it passes through the two-phase region.

*Quantitative Analysis of the $^2$H NMR Spectra of DPPC-$d_{62}$/Peptide 1.* The DPPC/$H_2O$ system is known to have a sharp phase transition between the gel and liquid-crystalline phases. The transition occurs near 41 °C for protiated DPPC/$H_2O$ and near 37 °C for DPPC-$d_{62}$/$H_2O$ (Davis, 1979). It is marked by a distinctive change in the shape and width of the $^2$H NMR spectrum. Comparison of Figure 6a with Figure 1 of Davis (1979) shows that the spectra of the DPPC-$d_{62}$/peptide 1 sample at $T \geq 44$ °C are similar to the liquid-crystalline spectra of the pure DPPC-$d_{62}$/$H_2O$ sample. For $T \leq 22$ °C, a comparison of Figure 6e with Figure 8 of Davis (1979) shows that the width of the $^2$H NMR spectra of the peptide-containing sample is similar to that of pure DPPC-$d_{62}$/$H_2O$ in the gel phase, though the lipid–peptide interaction does modify the shape somewhat.

The spectra between 44 and 22 °C can all be represented as superpositions of the characteristic liquid-crystalline- and gel-phase spectra. Thus, the range of coexistence of the gel and liquid-crystalline phases is extended from less than 1 °C for the pure DPPC-$d_{62}$/$H_2O$ (Davis, 1979) to about 20 °C when 2.3 mol % of peptide is present. It may be seen from Figure 6b that the gel-phase component of the $^2$H NMR spectrum is barely visible at 43 °C as a weak broad feature although it accounts for 12 ± 1% of the total $^2$H NMR intensity. On the other hand, the liquid-crystalline component is easily visible at 26 °C in Figure 6d because of its relative sharpness even though it comprises only about 3 ± 1% of the total spectral intensity. The spectrum at 39 °C, in which the gel distribution is 57 ± 4% of the intensity, is shown in Figure 6c.

The moment analysis leading to these estimates of the relative spectral intensities of the gel and liquid-crystalline phases will be described below. As we shall see, this analysis provides convincing quantitative evidence that the spectra between 44 and 22 °C can be accurately represented as a superposition of liquid-crystalline and gel spectra. Another demonstration of this point is the comparison of the "de-Paked" $^2$H NMR spectra for 45, 39, and 20 °C shown elsewhere (Davis et al., 1982), where it was seen that the 39 °C spectrum was a superposition of the other two spectra.

In order to analyze the $^2$H NMR spectra quantitatively, we conjecture that the normalized line shapes $F(\omega,T)$ at temperatures between 22 and 44 °C can be represented as a superposition of liquid-crystalline and gel line-shape functions $F_l(\omega,T)$ and $F_g(\omega,T)$ having fractional intensities $f$ and $1-f$, respectively, i.e.

$$F(\omega,T) = fF_l(\omega,T) + (1-f)F_g(\omega,T) \qquad (2)$$

We wish to analyze the spectra in the coexistence region quantitatively to obtain $f$ as a function of temperature. One method of estimating $f$ is to decompose the spectra visually into liquid-crystalline and gel components, guided by the spectral shapes of the pure phases. Such a procedure was used successfully in analyzing $^2$H NMR spectra in *Escherichia coli* membranes (Nichol et al., 1980). However, the relatively large

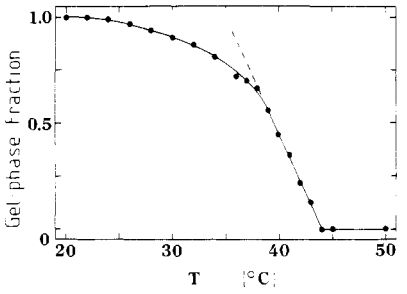


FIGURE 9: Fraction of DPPC-$d_{62}$ in the gel phase vs. temperature, determined by the moment analysis of the $^2$H NMR spectra of the 43:1 molar ratio sample of DPPC-$d_{62}$/peptide 1.

signal to noise ratio available with perdeuterated acyl chains can be more effectively exploited by the method of moments (Davis, 1979; Nichol et al., 1980; Davis et al., 1980; Bloom et al., 1978; Bienvenue et al., 1982; Jarrell et al., 1981).

The spectral moments, $M_n(T)$, eq 1, of a composite line satisfying eq 2 are related to the moments $M_n^l(T)$ and $M_n^g(T)$ of $F_l(\omega,T)$ and $F_g(\omega,T)$, respectively, by (Bienvenue et al., 1982)

$$M_n(T) = fM_n^l(T) + (1-f)M_n^g(T) \quad (3)$$

Plots of $M_1(T)$ vs. temperature for pure DPPC-$d_{62}$/$H_2O$ and for the peptide-containing sample were given in Figure 7. There is an inherent uncertainty in the extrapolation of $M_n^l(T)$ into the coexistence region from its variation with temperature for $T \geq 44$ °C and in the corresponding extrapolation for $M_n^g(T)$ from the results for $T \leq 22$ °C. In general, the moments in each phase depend on the peptide concentration; also, the partition of peptide molecules between the liquid-crystalline and gel phases is expected to vary in the coexistence region. In the case of *E. coli* membranes (Nichol et al., 1980), for example, it was found that although $M_1^l(T)$ and $M_2^l(T)$ varied approximately linearly with temperature in the pure liquid-crystalline phase, they were approximately independent of temperature in the coexistence region. This was also the *assumption* made by Jarrell et al. (1981) in their moment analysis of the partition of lipids between liquid-crystalline and gel phases of systems similar to those studied here. If one assumes that $M_1^l(T) = M_1^l(22\ °C)$ and $M_1^g(T) = M_1^g(44\ °C)$ for 22 °C < $T$ < 44 °C, analysis of the results of Figure 7 with eq 3 yields $f$ as a function of $T$ as plotted in Figure 9. We have tried other plausible extrapolation procedures for $M_1^l(T)$ [see, e.g., Davis (1979)] and found that they result in differences of about ±0.02, indicating that the deduced values of $f$ in Figure 9 are not sensitive to the extrapolation procedure used.

It should be noted that the upper and lower limits of the coexistence region are extremely well defined by our analysis. The definition of the upper limit, $T_U = 44$ °C, is accurately given by the linear variation of $f$, and hence $M_n(T)$, for temperatures just below $T_U$. The low temperature limit, $T_L = 22$ °C, is defined by the disappearance of the relatively sharp and easily detectable liquid-crystalline component.

A final check on the validity of our analysis is provided by the quantity

$$\Delta_2 = \frac{M_2}{1.35M_1^2} - 1 \quad (4)$$

which is the fractional mean-squared deviation of the quadrupolar splitting from the mean. The value of $\Delta_2$ in the gel phase at 22 °C is $\Delta_{2g} = 0.12$ and in the liquid-crystalline phase at 44 °C is $\Delta_{2l} = 0.16$. The predicted dependence of $\Delta_2$ on

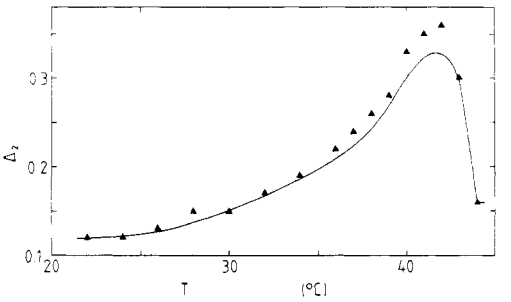


FIGURE 10: Parameter $\Delta_2 = M_2/(1.35M_1^2) - 1$ vs. temperature calculated from $^2$H NMR spectra of the 43:1 molar ratio sample of DPPC-$d_{62}$/peptide 1. In the liquid-crystalline phase, because of its axial symmetry, this parameter gives the relative mean-squared width of the distribution of quadrupolar splittings, while in the gel phase, $\Delta_2$ reflects the spread in the spectral intensity.

$f$ in the coexistence region may be expressed, by using eq 3, in terms of $\Delta_{2g}$, $\Delta_{2l}$, and $q = M_1^g/M_1^l$ as follows:

$$\Delta_2 = \frac{(1-f)q^2\Delta_{2g} + f\Delta_{2l} + f(1-f)(q-1)^2}{[(1-f)q + f]^2} \quad (5)$$

The predicted values of $\Delta_2$, by treating $\Delta_{2g}$, $\Delta_{2l}$, and $q$ as constants in the coexistence region and using the values of $f$ given in Figure 9, are compared with the values obtained directly from the $^2$H NMR spectra in Figure 10. Agreement is excellent considering that $\Delta_{2g}$, $\Delta_{2l}$ and $q$ are treated as constants.

Spectral simulations using the values of $f$ determined by the moment analysis can, in principle, be performed provided that a detailed model for the molecular motion of the gel-phase lipids can be found. Due to subtle variations in chain dynamics with chain position, the simulation of the spectra of specifically labeled rather than perdeuterated lipids would be more practical.

The observed phase behavior of the DPPC/peptide system and the values of the moments of the spectra both above and below the two-phase region, Figure 7, indicate that the present of the peptide strongly influences the behavior of the lipid molecules. It is clear that the peptide is intimately interacting with the lipids in both the gel and liquid-crystalline phase.

The average quadrupolar splitting, given by $M_1$, of the 43:1 molar ratio DPPC-$d_{62}$/peptide/water sample is only 5% larger than that of DPPC-$d_{62}$/water at 44 °C. By comparison, the 21% increase in the average quadrupolar splitting of the K-palmitate-$d_{31}$/peptide (100:1 mole ratio) sample over that of K-palmitate-$d_{31}$ at 49 °C is striking. A simple, approximate calculation of the average length of the K-palmitate chain, $\langle L \rangle$, by using the $^2$H quadrupolar splittings (Seelig & Seelig, 1974; Schindler & Seelig, 1975), indicates that the average bilayer thickness changes from approximately 27.3 Å for K-palmitate-$d_{31}$/water (70:30 by weight), which is in close agreement with X-ray measurements (Gallot & Skoulios, 1966), to a value of 29.1 Å at a K-palmitate-$d_{31}$/peptide mole ratio of 200:1 and a value of 34.0 Å at a mole ratio of 100:1. The X-ray diffraction measurements showed a change in repeat spacing from 38.2 to 40.7 Å. A 6.7-Å increase in bilayer thickness and only a 2.5-Å increase in total repeat spacing are only consistent if the thickness of the water layer decreases as peptide is added. That this is indeed the case was obvious upon inspection of the 100:1 mole ratio sample after centrifugation (performed during the sample preparation) since there was a clear bulk water layer at the bottom of the sample tube. In addition, the $^2$H NMR spectra of the samples with $^2H_2O$ contained an isotropic $^2H_2O$ peak instead of the powder pattern usually found in 70:30 mixtures of *K*-palmitate/$^2H_2O$ (Ab-

dollal et al., 1977). The effect of the peptide on the K-palmitate-$d_{31}$ bilayer is to dramatically increase the average molecular order, i.e., increase the average length of the palmitate chain, and expel much of the water from between the bilayers.

## Conclusions

The lipid/peptide model systems described here have already exhibited some interesting behavior. Our ability to modify the system should provide us with a broad understanding of the interactions among the different components of this model membrane.

We have recently begun to map out the phase diagram of this system using the techniques described here, systematically varying the peptide concentration. To investigate the importance of any mismatch between the length of the hydrophobic segment of the peptide and the bilayer thickness, we have synthesized shorter peptides, with 16 or 20 leucines, and are using phospholipids with different chain lengths.

The influence of the polar regions on the phase behavior of the system may be as significant as that of the hydrophobic core of the peptide. The lysine residues we have been using actually have an amphiphilic character of their own and can, by virtue of their four methylene segments, adjust their length to match the lipid bilayer to some degree. To investigate the effect of the polar part of the peptide, we are replacing the lysine residues with aspartic acid.

The behavior of the peptide in its lipid environment is also of interest. While the phase behavior of the combined system will describe the partitioning of the peptide among the different phases, to study the molecular order and dynamics of the peptides we need to look directly at the peptide itself. $^1$H NMR studies of the peptides in solution, as a dry powder, and in a completely deuterated lipid/$^2H_2O$ system have so far not provided much insight into the peptide's behavior (J. H. Davis, unpublished data). The $^1$H NMR spectrum in all of these cases is dominated by the numerous methyl groups on the molecule, and these are relatively insensitive to the subtle changes in molecular motion that may occur at physiological temperatures, e.g., near the gel to liquid-crystalline phase transition.

Experiments, using $^2$H NMR, wherein the amide hydrogens of the peptide backbone are exchanged for $^2$H are under way. In addition, samples of the peptide are being synthesized with $^2$H-labeled leucine. $^2$H NMR studies of these samples can provide us with detailed information on the orientational order and dynamics of the peptide in the lipid bilayer.

## Acknowledgments

We thank R. H. Stinson and J. C. Huschilt for help with the X-ray diffraction measurements and K. Vineberg for the circular dichroism work on the peptide in vesicles.

**Registry No.** $K_2L_{24}K_2A$-amide, 81116-03-2; $K_2GL_{24}K_2A$-amide, 86968-49-2; DPPC, 63-89-8; potassium palmitate, 2624-31-9.

## References

Abdollal, K., Burnell, E. E., & Valic, M. I. (1977) *Chem. Phys. Lipids 20*, 115–129.

Alter, J. E., Taylor, G. T., & Scheraga, H. A. (1972) *Macromolecules 5*, 739–745.

Bienvenue, A., Bloom, M., Davis, J. H., & Devaux, P. F. (1982) *J. Biol. Chem. 257*, 3032–3038.

Bloom, M., Davis, J. H., & Dahlquist, F. W. (1979) *XXth Ampere Congress Proceedings*, Tallinn, Estonia, Aug 1978, Springer-Verlag, Berlin, p 551.

Chen, S. C., Sturtevant, J. M., & Gaffney, B. J. (1980) *Proc. Natl. Acad. Sci. U.S.A. 77*, 5060–5063.

Chen, Y.-H., Yang, J. T., & Chou, C. H. (1974) *Biochemistry 13*, 3350–3359.

Chou, P. Y., & Fasman, G. D. (1977) *Trends Biochem. Sci. (Pers. Ed.) 2*, 128–131.

Davis, J. H. (1979) *Biophys. J. 27*, 339–358.

Davis, J. H. (1983) *Biochim. Biophys. Acta 737*, 117–171.

Davis, J. H., & Jeffrey, K. R. (1977) *Chem. Phys. Lipids 20*, 87–104.

Davis, J. H., Jeffrey, K. R., Bloom, M., Valic, M. I., & Higgs, T. P. (1976) *Chem. Phys. Lett. 42*, 390–393.

Davis, J. H., Bloom, M., Butler, K. W., & Smith, I. C. P. (1980) *Biochim. Biophys. Acta 597*, 477–491.

Davis, J. H., Hodges, R. S., & Bloom, M. (1982) *Biophys. J. 37*, 170–171.

Devaux, P. F. (1983) *Biol. Magn. Reson.* (in press).

Gallot, B., & Skoulios, A. (1966) *Kolloid Z. Z. Polym. 208*, 37–43.

Gupta, C. M., Radhakrishnan, R., & Khorana, H. G. (1977) *Proc. Natl. Acad. Sci. U.S.A. 74*, 4315–4319.

Henderson, R. (1981) *Membranes and Intercellular Communication* (Balian, R., Chabre, M., & Devaux, P. F., Eds.) pp 229–249, North-Holland, Amsterdam.

Hodges, R. S., & Merrifield, R. B. (1975a) *Anal. Biochem. 65*, 241–272.

Hodges, R. S., & Merrifield, R. B. (1975b) *J. Biol. Chem. 250*, 1231–1241.

Hsiao, C. Y. Y., Ohaway, C. A., & Wetlauter, D. B. (1974) *Lipids 9*, 913–916.

Jacobs, R. E., & Oldfield, E. (1981) *Prog. Nucl. Magn. Reson. Spectrosc. 14*, 113–136.

Jahnig, F., Harlos, K., Vogel, H., & Eibl, H. (1979) *Biochemistry 18*, 1459–1468.

Jarrell, H. C., Byrd, R. A., & Smith, I. C. P. (1981) *Biophys. J. 34*, 451–463.

Lewis, B. A., & Engelman, D. M. (1983) *J. Mol. Biol. 166*, 203–210.

McDonald, C. C., & Phillips, W. D. (1969) *J. Am. Chem. Soc. 91*, 1513–1521.

McLachlan, A. D., & Henderson, R. (1980) *Biochem. Soc. Trans. 8*, 677–678.

Nichol, C. P., Davis, J. H., Weeks, G., & Bloom, M. (1980) *Biochemistry 19*, 451–457.

Schindler, H., & Seelig, J. (1975) *Biochemistry 14*, 2283–2287.

Seelig, A., & Seelig, J. (1974) *Biochemistry 13*, 4839–4845.

Seelig, J., & Seelig, A. (1980) *Q. Rev. Biophys. 13*, 19–61.